Induction of Columnar Mesomorphism in Tetracoordinated Ionic Silver(I) Complexes Based on Chelate 4,4′-Disubstituted 2,2′-Bipyridines

Daniela Pucci,*[a] Giovanna Barberio,[a] Anna Bellusci,[a] Alessandra Crispini,[a] Massimo La Deda,[a] Mauro Ghedini,[a] and Elisabeta Ildyko Szerb[a]

Keywords: Bipyridine ligands / Silver / Metallomesogens / Ionic / Luminescence

The reaction of silver triflate (AgOTf) and silver dodecyl sulfate (AgDOS) with two nonmesomorphic 4,4′-disubstituted 2,2′-bipyridines, L^n, yielded a series of bis-chelate ionic silver complexes $[Ag(L^n)_2]X$. Complexation induced columnar mesomorphism in all the silver(I) tetra-branched bipyridine derivatives and the role of the counterion proved to be crucial in the generation of different symmetries of the mesophase. Remarkably, all silver(I) complexes exhibit emission at room temperature both in solution and in the solid state.

Introduction

Metallomesogens are a fascinating branch of nanostructure materials research,[1] as they join a current goal in supramolecular chemistry,[2] such as the self-assembly of coordinated species, with new functionalities provided from liquid crystalline properties.[3]

Our interest in this field has recently prompted us to employ nonmesogenic 4,4′-disubstituted 2,2′-bipyridines as building blocks in the synthesis of new coordination complexes, the mesomorphic properties of which are induced through the self-assembly of half-disc shaped $[LMCl_2]$ complexes (M = Pd, Pt, Ni, Zn) to full disc-shaped supramolecules, by the complementary shape approach. The complexes are liquid crystals regardless of the metal ion coordination geometry. The molecular organisation in the mesophase was mainly driven by intermolecular attractive interactions, with small structural variations having only subtle effects on the overall properties.[4]

Encouraged by these results, an electrostatic interaction was introduced to the molecular architecture and consequently to the supramolecular assembly. The synthesis of coordinatively saturated homoligand silver(I) complexes based on 2,2′-bipyridine ligands functionalised with amidic substituents in 4,4′-positions and with triflate as the counterion has been reported previously.[5] For the first time metallomesogens with tetracoordination around the silver(I) centre, based on chelate bipyridine ligands, were obtained. For these novel ionic liquid crystals a tetra-branched geometry induced mesomorphic molecular structures, such as columns. However, the presence of the amidic substituents introduced order in the structure, probably because of the ability to form H-bonding interactions, which lead to high transition temperatures.[5]

Novel examples of silver(I) complexes based on the nonmesomorphic 2,2′-bipyridines functionalised in 4,4′-positions with different substituents have been synthesised, as an alternative route to obtain low-temperature nonconventional ionic thermotropic metallomesogens. Four cationic bis-chelate silver complexes $[Ag(L^n)_2]X$ (Scheme 1) displaying columnar mesomorphism induced upon complexation are described here. These complexes are mesogenic even though they show pseudo-tetrahedral geometry around the metal centre, which would usually prevent the appearance of mesomorphic behaviour.[6]

The synthesis of metal complexes represents a challenge for obtaining new functional liquid crystalline materials where a wide choice of combinations of both metals and ligands would enhance preselected properties such as charge transport or luminescence.[1] Among the few reports on photoactive metallomesogens, few systems involve the use of the silver(I) ion,[7] although the various coordination modes of Ag^I, combined with the presence within the Ag complexes of large π systems as ligands,[8] would represent an ideal mode to expand the applicability of metallomesogens in the field of electro-optics.

Because many practical applications require liquid crystalline materials luminescent at room temperature, our investigations have reached this goal, giving rise to silver(I) complexes which exhibit emission at room temperature.

Moreover, the effect of the triflate (OTf) and the dodecyl sulfate (DOS) counterions on the mesogenic and photophysical properties have been investigated.

In the description of the $[Ag(L^n)_2]X$ complexes, dendrimeric terminology has been used in order to distinguish be-

[a] Centro di Eccellenza CEMIF.CAL-LASCAMM, Unità INSTM della Calabria, Dipartimento di Chimica, Università della Calabria,
87030 Arcavacata (CS), Italy

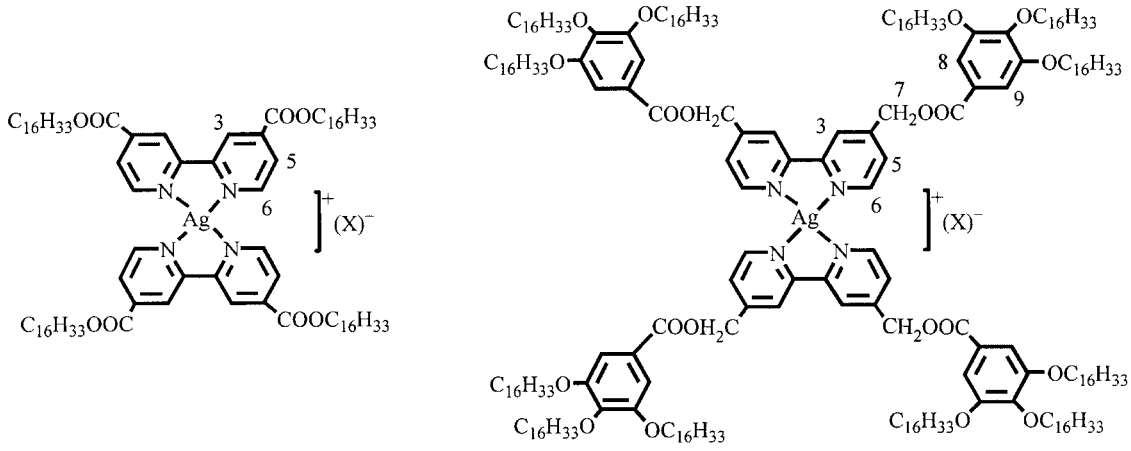

Scheme 1.

tween the different types of substituents on the bipyridine cores. Therefore all the silver derivatives are referred to as first-generation tetra-branched compounds, and the L^2 derivatives, **3** and **4**, as second-generation 12-branched compounds (Scheme 2).

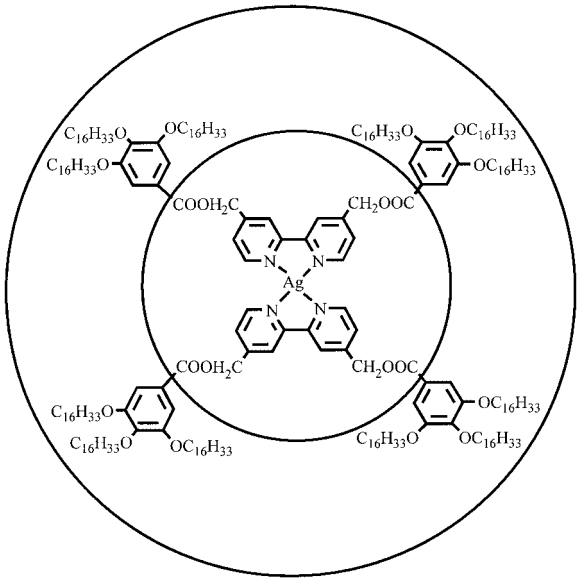

Scheme 2.

Results and Discussion

Synthesis

The reaction of L^n ligands with the appropriate silver salts (AgOTf and AgDOS) in a 1:2 metal-to-ligand stoichiometry, in dichloromethane, led to the formation of $[Ag(L^n)_2][X]$ complexes, **1**–**4**, in very good yields. The stoichiometry and purity of all compounds were confirmed using elemental analyses, IR and ^1H NMR spectroscopy. In these cationic bis-chelate silver derivatives, the silver atom is in a distorted tetrahedral geometry coordinated by four nitrogen atoms of the two bipyridines, as already found in the crystal structure determination of nonsubstituted 2,2′-bipyridine silver complexes with anions such as $(BF_4)^-$ and $(PF_6)^-$.[9,10]

Liquid Crystalline and Photophysical Properties

Although the ligands L^n are not liquid crystals, the complexation to different silver salts gave rise to the new series of complexes, **1**–**4**, which all showed thermally reproducible mesomorphism, characterised by a combination of optical microscopy (POM), differential scanning calorimetry (DSC) and powder X-ray diffraction analysis at variable temperature (PXRD). The thermal data of the $[Ag(L^n)_2]X$ series are summarised in Table 1 and the relative phase diagram is reported in Figure 1.

All the complexes **1**–**4** showed, after a crystal-to-crystal transition, enantiotropic columnar phases, with melting temperatures under 100 °C. The results from POM suggested, for both triflate complexes (**1** and **3**), the presence of a hexagonal mesophase with the typical fan-shaped optical texture with homeotropic areas (Plate 1 in Figure 2). As regards the dodecyl sulfate derivatives (**2** and **4**), they exhibit a different optical behaviour: for complex **2**, a texture with Maltese crosses appeared after annealing on cooling from the isotropic melt, which developed in the fingerprint texture reported in Figure 2 (plate 2); while complex **4** exhibits a fine columnar fan-like texture (plate 3 in Figure 2).

The columnar nature of the mesophases shown by complexes **1**–**4** has been confirmed by PXRD at variable temperature; the X-ray diffraction data are listed in Table 2.

The XRD patterns of the triflate complexes, **1** and **3**, are typical of a two-dimensional hexagonal lattice with the three peaks in the low angle region in the ratio $1:(3)^{1/2}:2$. In both cases, the wide angle region displayed a broad halo centred at 4.6–4.7 Å, typical of liquid-like correlations be-

Table 1. Optical and thermal data of complexes **1**–**4**.

Complex[a]	Transition[a]	T/°C[a]	ΔH/kJ mol^{-1}
$[Ag(L^1)_2](OTf)$ (**1**)	Cr–Cr′	33	14.4
	Cr′–Col_h	59	8.14
	Col_h–I	71	56.7
	I–Col_h + Cr[b]	48	44.3
$[Ag(L^1)_2](DOS)$ (**2**)	Cr–Cr′	77	16.8
	Cr′–Col_r	81	98.5
	Col_r–I	85	62.2
	I–Col_r	64	41.2
	Col_r–Cr	48	39.3
$[Ag(L^2)_2](OTf)$ (**3**)	Cr–Cr′	49	111.9
	Cr′–Col_h	69	10.0
	Col_h–I	97	3.3
	I–Col_h	96	3.2
	Col_h–Cr	44	118.7
$[Ag(L^2)_2](DOS)$ (**4**)	Cr–Cr′	58	85.0
	Cr′–Col_r	77	34.9
	Col_r–I	90	2.3
	I–Col_r + Cr[b]	55	135.2

[a] Cr: crystal; Col: columnar; I: isotropic liquid. [b] Only a broad peak for the two transitions.

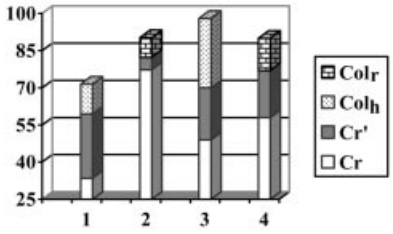

Figure 1. Phase diagram of complexes **1**–**4**.

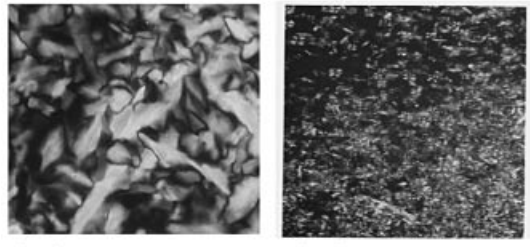

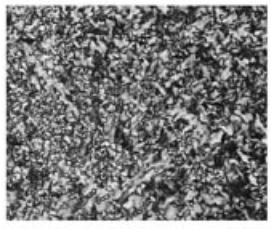

Figure 2. Polarised light optical photomicrograph of the textures exhibited by complex **3** at 85 °C on cooling (Plate 1); by complex **2** at 60 °C on cooling (Plate 2); and by complex **4** at 85 °C on heating (Plate 3).

Table 2. X-ray diffraction data of complexes **1**–**4**.

Complex	Mesophase lattice constants/Å	$d_{obsd.}$/Å ($d_{calcd.}$/Å)	Miller indices
1		43.7 (43.7)	(1 0)
	Col_h at 68 °C	26.6 (25.2)	(1 1)
	(on heating)	22.2 (21.8)	(2 0)
		14.8 (14.3)	(3 0)
	a = 51.6	ca. 4.7	broad
	n = 3.0[a]	ca. 3.6	broad
2		38.7 (38.7)	(1 1)
	Col_r at 83 °C	29.1 (29.1)	(2 0)
	(on heating)	19.2 (19.3)	(2 2)
		12.9 (12.9)	(0 4)
	a = 58.3	4.6	
	b = 51.6	4.3	
		4.0	
3		37.3 (37.3)	(1 0)
	Col_h at 86 °C	21.4 (21.5)	(1 1)
	(on cooling)	18.9 (18.6)	(2 0)
		ca. 4.6	broad
	a = 43.2		
	n = 1.1[a]		
4		48.4 (48.4)	(2 0)
	Col_r at 84 °C	36.5 (36.5)	(1 1)
	(on heating)	25.2 (25.0)	(3 1)
		20.7 (20.6)	(4 1)
	a = 96.8	16.6 (16.8)	(3 2)
	b = 39.4	ca. 4.7	broad
		ca. 4.1	broad

[a] Number of molecules calculated according to the formula $n = V_{cell}(N_A/M)\rho$ assuming a density of 1 g cm^{-3}, where N_A is the Avogadro constant; V_{cell} is calculated assuming a height of 3.6 Å for **1** and 4.6 Å for **3**.

tween side chains, while only in the case of complex **1** is a peak present at 3.6 Å, corresponding to the distance between adjacent cores. These differences account for a more ordered hexagonal phase in the case of complex **1**, in which there is a reduced number of aliphatic peripheral chains around the central core. The crystallinity of the mesophase in this case is also confirmed by the huge difference in the transition enthalpy values for the Col_h–I transitions of **1** and **3**, as reported in Table 1. Remarkably, the lattice parameter of **1** (a_{hex} = 51.6 Å) is significantly greater than that of complex **3** (a_{hex} = 43.2 Å), which has bulkier substituents on the 2,2′-bipyridines and greater side-chain density. This difference, which has already been observed in other polycatenar compounds with variable length alkyl chains,[11] reflects the different organisation of the molecules within the columns depending on the number of the alkyl chains. For the Col_h phase of **1**, approximately three molecules instead of just the one calculated for complex **3** can be found in the cross-section of the columns when the height of the columnar slice is assumed to be 4.6 Å (Table 2), indicating that the overall organisation between the molecular cores is of an edge-to-edge type. In the case of the second-generation 12-branched complex **3**, the four phenyl rings and 12 chains per molecule can completely sur-

round the molecular cores, reducing the number of molecules in the cross-section of each unit cell.

The symmetry of the columnar mesophases changes on going from the OTf to the DOS derivatives. In fact, both DOS derivatives **2** and **4** showed X-ray diffraction patterns of a rectangular columnar mesophase, characterised by two sharp fundamental peaks in the low angle region (Figure 3).

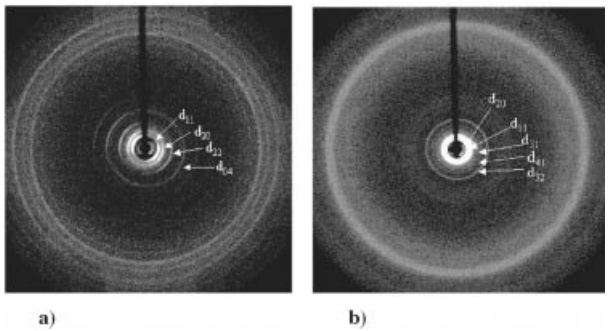

Figure 3. X-ray diffraction patterns of nonaligned samples of the rectangular columnar phases of (a) complex **2** at 87 °C on heating and (b) complex **4** at 84 °C on heating.

.

The change in the shape of the counterion destabilises the hexagonal phase, favouring rectangular phases at higher temperatures. The mesophase crossover from Col_r to Col_h is generally associated with the increase of the side-chain lengths or with the different size of the metal centres,[5,12,13] and, in both cases, the effect is a greater core–core interaction, which favours the formation of the Col_r phase. In a Col_h phase a rotationally averaged shape of the molecules gives a circular projection along the column's axis and the mesogenic plane is perpendicular to the column's axis. A distortion from Col_h to a Col_r is obtained when the molecules project an elliptical shape along the column's axis (Figure 4).[14]

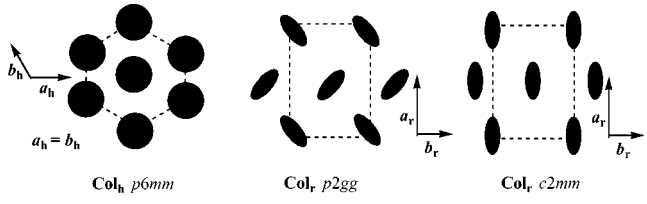

Figure 4. Schematic representation of the 2D lattices of the different columnar mesophases observed and their associated plane groups.

In this case the presence of the DOS counterion, which because of its shape can be organised with the flexible aliphatic chain aligned in the direction of the aliphatic periphery of the cation, hinders the molecular rotation of the nondisclike molecules, generating an elliptical cross-section. Within the rectangular arrangements, two different symmetries characterised by two different plane groups can be distinguished. The indexation of the two spectra showed that the reflection conditions for the *c2mm* plane group are verified in the case of complex **2**, with the (11) reflection being at a smaller angle ($d_{11} > d_{20}$), while the *p2gg* plane group is assigned to the Col_r phase of the second-generation 12-branched complex **4** (Table 2). Indeed the presence of a further aliphatic chain of the DOS counterion induces a more pronounced effect on the second-generation tetrabranched complex **2** with respect to the second-generation 12-branched complex, in which the volume fraction of the flexible chains completely surrounds the polar inner sphere.

Another important feature of the two rectangular columnar mesophases is the notable difference in the organisation within the columns evidenced by the high angle region of the XRD spectra. While in the XRD spectrum of **4** only a broad halo centred at 4.7 Å is present, typical of liquid-like correlations between side chains; in the case of **2**, three distinct reflections are observable at 4.6, 4.3 and 4.0 Å, indicative of a crystalline rectangular mesophase (Figure 3). This is confirmed also by the difference in the enthalpy values associated with the transitions to the isotropic liquid (Table 1).

A photophysical study has been performed on compounds **1**–**4**, in dichloromethane solution at room temperature, to assess the absorption and luminescence properties of the single subunits (Table 3).

The absorption features of the ligands are very similar to each other, and characteristics of these chromophores:[4b] π–π* excitations on aromatic rings give rise to two main bands at 240 and 300 nm (Table 3), which appear with a shoulder because of a vibrational progression. A weak low-energy band at about 330 nm is assigned to an n–π* transition. In the L^2 spectrum some differences are found: in particular, the band maximum at 278 nm is blue-shifted and more intense with respect to the corresponding band in L^1; this is attributed to the introduction of three hexadecyloxybenzyl substituents which stabilise the π orbital on the pyridine ring by exerting a weak electron-donating effect. Moreover, the aromatic transitions localised on the phenyl rings of the substituents contribute to the intensity of the

Table 3. Photophysical data.

Compound	Solution Abs., λ/nm (ε/L mol^{-1} cm^{-1})[a]	Em, λ/nm (Φ)	Solid Abs., λ/nm	Em, λ/nm
1	250 (sh), 275 (sh), 310 (21000), 315 (sh), 330 (sh)	350 (1.0%)	310, 320	350
2	250 (sh), 275 (sh), 310 (16800), 315 (sh), 330 (sh)	350 (0.8%)	310, 320, 340	365
3	250 (sh), 280 (66270), 290 (sh)	355 (3.5%)	280	367
4	250 (sh), 280 (82860), 290 (sh)	355 (3.0%)	280	367

[a] sh: shoulder.

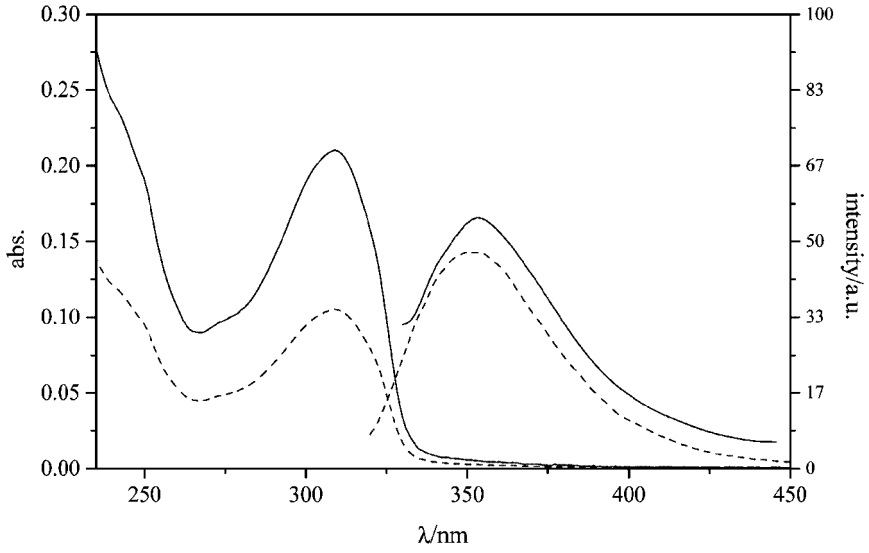

Figure 5. Absorption and emission spectra of **1** (solid line) and **3** (dashed line) in dichloromethane solution.

278-nm band. Metal complexation of both ligands induces a slight red-shift of the absorption bands in their derivatives (Figure 5), while, as expected, in solution no appreciable spectral differences are attributed to the influence of the two counterions. In the spectra of complexes **1** and **2** a weak band is visible at 275 nm, attributed to a ligand-to-metal-charge transfer;[15] the same feature in the spectra of **3** and **4** is probably hidden by the intense band at 278 nm.

The emission spectra of the ligands show a maximum at 350 (L^1) and 355 nm (L^2), which is ascribable to the deactivation of the π–π*-related state (Table 3); the measured quantum yields are comparable with those found for similar compounds.[4b] All the first-generation tetra-branched complexes showed the same luminescence observed in their corresponding ligands,[4b] and attributed to a ^{1}LC (ligand centred) transition. The observed quantum yields for these complexes are reduced because of the presence of the heavy atoms which induce $^1LC \rightarrow {}^3LC$ intersystem crossing.[16] In solution, no spectral differences are attributable to the counterion and the differences among Φ-values of the L^1 and L^2 derivatives are within the range of experimental uncertainty. Remarkably, in analogy to the corresponding ligands, the second-generation 12-branched complexes **3** and **4** have a quantum yield higher than that of complexes **1** and **2**.

A study of the photophysical properties of both ligands and complexes **1**–**4** has been performed also in the solid state, with the intention of examining the influence of the crystal packing on the luminescence features. No significant differences have been recorded with respect to the spectra in solution (Table 3).

Conclusions

The general preference of the silver(I) ion in liquid crystals reported to date is for linear 2-coordination or for tetra-coordination in macrocycle derivatives.[1,17] However, often the structure and packing of the ionic silver complexes are influenced by the argentophilic interaction (Ag–Ag contacts) and by the presence of coordinating counterions, which can induce the coordination number to increase up to six. This change in the network dimensionality has led to a drawback for the silver complexes, namely that their high clearing temperatures and their poor thermal stability have meant that their physical properties have been scarcely investigated.

We have recently reported a new class of chelate silver bipyridine with a coordinative saturation around the metal centre. These complexes exhibited columnar mesomorphism at very high temperatures, as the presence of amidic functionalities on the bipyridine ligands gives rise to H-bonding interactions.[5] In order to overcome this structural limitation new ligands with different substituents have been used for the synthesis of a novel class of ionic $[Ag(L^n)_2][X]$ complexes with a tetracoordination around the silver centre. The coordination of the two nonmesomorphic ligand units, with different molecular features, namely rod-like for L^1 and hemi-disc for the hexacatenar L^2, to the silver atom gives rise to a starlike molecular shape because of the pseudo-tetrahedral coordination around the metal centre, and induces liquid crystalline behaviour in the resulting complexes. In particular, it seems that the difference in the molecular anisotropy and the volume of the cationic cores of the two ligands L^n does not perturb the molecular arrangement and the mesophase induction. Thus, all complexes show columnar mesomorphism, regardless of the nature and number of branchings on the organic ligand with a lowering by 100–200 °C of the clearing temperatures with respect to the similar amidic Ag^I complexes.[5]

However, the enhancement of the aliphatic periphery in the second-generation 12-branched compounds allows the transition from crystalline to liquid crystalline mesophases.

The symmetry of the mesophase of the four derivatives strongly depends on the structural role of the counterion, which drives the organisation of both the single molecular units and of the overall supramolecular motifs. Indeed the triflate anion has been found to promote the hexagonal phase while rectangular phases seem to be stabilised by the dodecyl sulfate anion which, because of its shape, can be organised with the flexible aliphatic chain aligned in the direction of the aliphatic periphery of the cation, hindering the molecular rotation of the nondisclike molecules and thus generating an elliptical cross-section. This change of mesophase morphology is related to the balance between the two microsegregate regions of the molecules, as evidenced by the different perturbation induced by the DOS anion on the two derivatives. Indeed for the second-generation 12-branched complex **4**, in which the volume fraction of the flexible chains completely surrounds the polar inner sphere, the presence of the aliphatic chain of the DOS counterion induces a less pronounced effect on the symmetry (*p2gg* lattice) than that on complex **2** (*c2mm* lattice).

The influence of the counteranion on thermal behaviour follows the same trend: the molecular arrangement in the solid phase of the dodecyl sulfate derivatives is more effective than that of the triflate complexes, which tend to melt at lower temperatures and show a wider mesophase range with respect to the homologues in the dodecyl sulfate series.

Moreover, complexes **1**–**4** show luminescence at room temperature both in solution and in the solid state, which is not a common feature for Ag^{I} derivatives,[8] and therefore they represent interesting materials for applicative purposes requiring room temperature luminescent liquid crystals.

Experimental Section

Materials and Measurements: Silver triflate (AgOTf) was purchased from Aldrich and used as received. Also the solvents were used as received from commercial sources without further purification. Ligands, dihexadecyl 2,2′-bipyridine-4,4′-dicarboxylate (L^1) and 4,4′-bis(3,4,5-trihexadecyloxybenzoyloxymethyl) 2,2′-bipyridine (L^2) were synthesised as previously reported.[4a,4c]

Infrared spectra were recorded with a Spectrum One FT-IR Perkin–Elmer spectrometer and ^{1}H NMR spectra with a Bruker AVANCE-300 spectrometer, in $CDCl_3$ solution, with TMS as internal standard. Elemental analyses were performed with a Perkin–Elmer 2400 analyser.

The textures of the mesophases were studied with a Zeiss Axioscope polarising microscope equipped with a Linkam CO 600 heating stage. The transition temperatures and enthalpies were measured with a Perkin–Elmer Pyris 1 Differential Scanning Calorimeter with a heating and cooling rate of 10 °C/min. The apparatus was calibrated with indium. Two or more heating/cooling cycles were performed on each sample.

Spectrofluorimetric grade dichloromethane (Acros Organics) was used for the photophysical investigations in solution, at room temperature. A Perkin–Elmer Lambda 900 spectrophotometer was employed to obtain the absorption spectra, while the uncorrected emission spectra, all confirmed by excitation ones, were recorded with a Perkin–Elmer LS 50B spectrofluorimeter, equipped with a Hamamatsu R928 photomultiplier tube. Emission quantum yields were determined using the optically dilute method[18a] on aerated solutions with absorbance at excitation wavelengths <0.1; $Ru(bipy)_3Cl_2$ (bipy = 2,2′-bipyridine) in water was used as standard (Φ = 0.028).[18b] The experimental uncertainty on the molar extinction coefficients is 10%, while on the emission quantum yields it is 15%. The examined compounds are fairly stable in dichloromethane, as demonstrated by the constancy of their absorption spectra over a week.

The powder X-ray diffraction patterns were obtained by using a Bruker AXS General Area Detector Diffraction System (D8 Discover with GADDS) with Cu-K_α radiation; the high sensitive area detector was placed at a distance from the sample of 10 cm and equipped with a CalCTec (Italy) heating stage. The samples were heated at a rate of 5.0 °C min^{-1} to the appropriate temperature. Measurements were performed by charging samples in Lindemann capillary tubes with an inner diameter of 0.5 mm.

Synthesis of Complexes: All silver complexes were prepared in a similar fashion from the appropriate ligands and silver salts. The synthesis of complex **1** is described in detail below while for all others only yields, ^{1}H NMR, IR and elemental analysis data are reported.

Bis(dihexadecyl 2,2′-bipyridyl-4,4′-dicarboxylate)silver(I) Triflate [$(L^1)_2$Ag](OTf) (1): A solution of AgOTf (15 mg, 0.0575 mmol) and L^1 (80 mg, 0.115 mmol) in dichloromethane (10 mL) was stirred under nitrogen (24 h, 40 °C), with the vessel protected from light. The mixture was then filtered through Celite and concentrated under reduced pressure. The product was collected as a yellow solid in 96% yield (90 mg) after precipitation by diethyl ether; thermotropic behaviour is shown in Table 1. ^{1}H NMR (300 MHz, $CDCl_3$, 25 °C, TMS): δ = 0.87 (t, $^3J_{H,H}$ = 6.4 Hz, 12 H, CH_3), 1.25 (m, 104 H, $(CH_2)_{13}CH_3$), 1.84 (m, 8 H, $CH_2(CH_2)_{13}CH_3$), 4.43 (t, $^3J_{H,H}$ = 6.8 Hz, 8 H, OCH_2), 8.07 (d, $^3J_{H,H}$ = 5.1 Hz, 4 H, H-5), 8.81 (s, 4 H, H-3), 8.92 (d, $^3J_{H,H}$ = 5.1 Hz, 4 H, H-6). IR (KBr): $\tilde{\nu}$ = 1726 cm^{-1} (C=O), 1288, 1255 cm^{-1} (OTf). $C_{89}H_{144}AgF_3N_4O_{11}S$ (1643.07): calcd. C 65.06, H 8.83, N 3.41; found C 65.16, H 8.90, N 3.34.

Bis(dihexadecyl 2,2′-bipyridyl-4,4′-dicarboxylate)silver(I) Dodecyl Sulfate [$(L^1)_2$Ag](DOS) (2): The product was collected as a pale yellow solid in 82% yield (83 mg); thermotropic behaviour is shown in Table 1. ^{1}H NMR (300 MHz, $CDCl_3$, 25 °C, TMS): δ = 0.87 (t, $^3J_{H,H}$ = 6.8 Hz, 15 H, CH_3), 1.25 (m, 122 H, $(CH_2)_nCH_3$), 1.84 (m, 10 H, $CH_2(CH_2)_nCH_3$), 4.10 (t, $^3J_{H,H}$ = 6.8 Hz, 2 H, O_3SOCH_2), 4.45 (t, $^3J_{H,H}$ = 6.6 Hz, 8 H, OCH_2), 8.10 (dd, $^3J_{H,H}$ = 5.1, $^4J_{H,H}$ = 1.5 Hz, 4 H, H-5), 8.86 (s, 4 H, H-3), 9.07 (d, $^3J_{H,H}$ = 5.1 Hz, 4 H, H-6). IR (KBr): $\tilde{\nu}$ = 1720 cm^{-1} (C=O), 1254, 1230 cm^{-1} (DOS). $C_{100}H_{169}AgN_4O_{12}S$ (1759.39): calcd. C 68.27, H 9.68, N 3.18; found C 68.33, H 9.58, N 3.05.

Bis[4,4′-bis(3,4,5-trihexadecyloxybenzoyloxymethyl)-2,2′-bipyridyl]-silver(I) Triflate [$(L^2)_2$Ag](OTf) (3): The product was collected as a white solid in 92% yield (211 mg); thermotropic behaviour is shown in Table 1. ^{1}H NMR (300 MHz, $CDCl_3$, 25 °C, TMS): δ = 0.85 (t, $^3J_{H,H}$ = 6.2 Hz, 36 H, CH_3), 1.25 (m, 312 H, $(CH_2)_{13}CH_3$), 1.83 (m, 24 H, $CH_2(CH_2)_{13}CH_3$), 4.02 (t, $^3J_{H,H}$ = 6.8 Hz, 24 H, OCH_2), 5.53 (s, 8 H, H-7), 7.32 (s, 8 H, H-8,9), 7.57 (d, $^3J_{H,H}$ = 4.9 Hz, 4 H, H-5), 8.32 (s, 4 H, H-3), 8.64 (d, ^3J = 5.0 Hz, 4 H, H-6). IR (KBr): $\tilde{\nu}$ = 1709 cm^{-1} (C=O), 1252, 1220 cm^{-1} (OTf). $C_{245}H_{424}AgF_3N_4O_{23}S$ (3991.00): calcd. C 73.73, H 10.71, N 1.40; found C 73.52, H 10.56, N 1.41.

Bis[4,4′-bis(3,4,5-trihexadecyloxybenzoyloxymethyl)-2,2′-bipyridyl]-silver(I) Dodecyl Sulfate, [$(L^2)_2$Ag](DOS) (4): The product was collected as a beige solid in 78% yield (184 mg); thermotropic behav-

iour is shown in Table 1. ^{1}H NMR (300 MHz, $CDCl_3$, 25 °C, TMS): δ = 0.89 (t, $^3J_{H,H}$ = 6.6 Hz, 39 H, CH_3), 1.27 (m, 330 H, $(CH_2)_nCH_3$), 1.79 (m, 26 H, $CH_2(CH_2)_nCH_3$), 4.04 (m, 26 H, OCH_2), 5.51 (s, 8 H, H-7), 7.34 (s, 8 H, H-8,9), 7.48 (d, $^3J_{H,H}$ = 5.1 Hz, 4 H, H-5), 8.43 (s, 4 H, H-3), 8.70 (d, ^3J = 5.1 Hz, 4 H, H-6). IR (KBr): $\tilde{\nu}$ = 1709 cm^{-1} (C=O), 1254, 1221 cm^{-1} (DOS). $C_{256}H_{449}AgN_4O_{24}S$ (4107.32): calcd. C 74.86, H 11.02, N 1.36; found C 75.05, H 10.97, N 1.61.

Acknowledgements

This work was partly supported by the Italian Ministero dell′Istruzione, dell′Università e della Ricerca (MIUR) through the INSTM-FIRB and Centro di Eccellenza CEMIF.CAL grants.

[1] a) J. L. Serrano, *Metallomesogens*, Wiley-VCH, Weinheim, **1996**; b) B. Donnio, D. W. Bruce, "Metallomesogens" in *Structure and Bonding* vol. 95 (Liquid Crystals II) (Ed.: D. M. P. Mingos), Springer, Heidelberg, **1999**; c) B. Donnio, D. Guillon, R. Deschenaux, D. W. Bruce, "Metallomesogens" in *Comprehensive Coordination Chemistry II*, vol. 6 (Eds.: J. A. McCleverty, T. J. Meyer), Elsevier, Oxford, **2003**.

[2] J. M. Lehn, *Science* **2002**, *295*, 2400–2415.

[3] T. Kato, N. Mizoshita, *Curr. Opin. Sol. State Mater. Sci.* **2002**, *6*, 579–587.

[4] a) D. Pucci, G. Barberio, A. Crispini, O. Francescangeli, M. Ghedini, *Mol. Cryst. Liq. Cryst.* **2003**, *395*, 155–165; b) D. Pucci, G. Barberio, A. Crispini, O. Francescangeli, M. Ghedini, M. La Deda, *Eur. J. Inorg. Chem.* **2003**, 3649–3661; c) G. Barberio, A. Bellusci, A. Crispini, M. Ghedini, A. Golemme, P. Pruss, D. Pucci, *Eur. J. Inorg. Chem.* **2005**, 181–188.

[5] D. Pucci, G. Barberio, A. Bellusci, A. Crispini, M. Ghedini, E. I. Szerb, *Mol. Cryst. Liq. Cryst.* **2005**, in press.

[6] A. Pegenau, T. Hegmann, C. Tschierske, S. Diele, *Chem. Eur. J.* **1999**, *5*, 1643–1651.

[7] P. K. Sudhadevi Antharjanam, V. Ajay Mallia, S. Das, *Chem. Mater.* **2002**, *14*, 2687–2692.

[8] a) X.-C. Huang, S.-L. Zheng, J.-P. Zhang, X.-M. Chen, *Eur. J. Inorg. Chem.* **2004**, 1024–1029; b) Y. Kang, C. Seward, D. Song, S. Wang, *Inorg. Chem.* **2003**, *42*, 2789–2797.

[9] E. C. Constable, C. E. Housecroft, M. Neuburger, I. Poleschak, M. Zehnder, *Polyhedron* **2003**, *22*, 93–108.

[10] H.-P. Wu, C. Janiak, G. Rheinwald, H. Lang, *J. Chem. Soc. Dalton Trans.* **1999**, 183–190.

[11] T. Hegmann, J. Kain, S. Diele, B. Schubert, H. Bögel, C. Tschierske, *J. Mater. Chem.* **2003**, *13*, 991–1003.

[12] C. K. Lai, C.-H. Tsai, Y.-S. Pang, *J. Mater. Chem.* **1998**, *8*, 1355–1360.

[13] H. Zheng, C. K. Lai, T. M. Swager, *Chem. Mater.* **1995**, *7*, 2067–2077.

[14] D. Goldmann, D. Janietz, C. Schmidt, J. H. Wendorff, *J. Mater. Chem.* **2004**, *14*, 1521–1525.

[15] a) V. W. W. Yam, *Pure Appl. Chem.* **2001**, *73*, 543–548; b) C. R. Wang, K. K. W. Lo, V. W. W. Yam, *Chem. Phys. Lett.* **1996**, *262*, 91–96.

[16] N. Armaroli, M. A. J. Rodgers, P. Ceroni, V. Balzani, C. O. Dietrich-Buchecker, J. M. Kern, A. Bailal, J. P. Sauvage, *Chem. Phys. Lett.* **1995**, *241*, 555–558.

[17] F. Neve, *Adv. Mater.* **1996**, *8*, 277–289.

[18] a) J. N. Demas, G. A. Crosby, *J. Phys. Chem.* **1971**, *75*, 991–1024; b) K. Nakamaru, *Bull. Soc. Chem. Jpn.* **1982**, *5*, 2697–2705.

Received: January 03, 2005

